

MP 00W0000138

MITRE PRODUCT

An Overbound Concept for Pseudorange Error from the LAAS Ground Facility

July 2000

Curtis A. Shively
Ronald Braff

© 2000 The MITRE Corporation

MITRE
Center for Advanced Aviation System Development
McLean, Virginia



This paper was presented at the Annual Meeting of the Institute of Navigation in San Diego, California, 26–28 June 2000.

MP00W0000138

MITRE PRODUCT

An Overbound Concept for Pseudorange Error from the LAAS Ground Facility

July 2000

Curtis A. Shively
Ronald Braff

Sponsor: Federal Aviation Administration
Dept. No.: F082

Contract No.: DTFA01-93-C-00001
Project No.: 02001403-LS

The contents of this material reflect the views of the Center for Advanced Aviation System Development. Neither the Federal Aviation Administration nor the Department of Transportation makes any warranty or guarantee, or promise, expressed or implied, concerning the content or accuracy of the views expressed herein.

Approved for public release; distribution unlimited.

©2000 The MITRE Corporation

MITRE

**Center for Advanced Aviation System Development
McLean, Virginia**

MITRE Department
and Project Approval:

Melvin J. Zeltser
Program Manager
Navigation and Surveillance

© 2000 The MITRE Corporation. All rights reserved.

This is the copyright work of The MITRE Corporation and was produced for the U.S. Government under Contract Number DTFA01-93-C-00001 and is subject to Federal Acquisition Regulation Clause 52.227-14, Rights in Data-General, Alt. III (JUN 1987) and Alt. IV (JUN 1987). No other use other than that granted to the U.S. Government, or to those acting on behalf of the U.S. Government, under that Clause is authorized without the express written permission of The MITRE Corporation. For further information, please contact The MITRE Corporation, Contracts Office, 1820 Dolley Madison Blvd., McLean, VA 22102, (703) 883-6000.

Abstract

The FAA's Local Area Augmentation System (LAAS) broadcasts a parameter σ_{pr_gnd} to describe the errors in the differential corrections due to the LAAS ground facility (LGF). An aircraft using LAAS computes a high probability bound on the resulting error in the position domain based on σ_{pr_gnd} assuming that the errors are Gaussian distributed. This paper proposes a method for characterizing the ground error distribution and ensuring a bound is provided if the tails of the error are not Gaussian. The proposed probability density function (PDF) for the ground error is synthesized from a Gaussian core and Laplacian tails. Hypothesis tests are developed for verifying error probability density and tail probability values from data. The degree to which these parameters can be verified with known confidence is derived as a function of the number of independent samples and the point on the error distribution where the tail is defined. Use of the Laplacian tail and the uncertainties in the parameters because of limited availability of data require that the estimated value of σ_{pr_gnd} be inflated before broadcast to ensure the bound is achieved in the aircraft. Results show that even if thousands of independent samples are used, the inflation factors (INFs) needed are significantly larger than if the tails of the error distribution are known to be Gaussian.

Acknowledgments

The authors wish to thank Maria DiPasquantonio and Ted Urda of the FAA LAAS Program for sponsoring this research.

Table of Contents

| Section | Page |
|---|-------------|
| 1. Introduction | 1 |
| Background | 1 |
| Purpose and Organization of This Paper | 2 |
| 2. Collecting Data to Characterize Probabilities | 3 |
| Independent Samples of LAAS Error | 3 |
| Chance of Observing Rare Values | 4 |
| 3. Overview of Proposed Bounding Method | 5 |
| 4. Model For Error of Single Reference Receiver | 7 |
| Steps in Generation and Verification | 7 |
| Idealized Error Model Probability Density Function | 8 |
| 5. Hypothesis Tests | 9 |
| General Performance Characteristics | 9 |
| Probability Uncertainties That Can Be Verified | 10 |
| Verifiable Error Model Probability Density Function | 13 |
| 6. Inflation Factor Results | 15 |
| Example of Cumulative Distribution Function (Tail) Bounding | 15 |
| Variation of Inflation Factor with Number of Samples | 16 |
| Variation of Inflation Factor with Confidence | 17 |
| 7. Summary | 19 |
| 8. Recommendations | 21 |
| List of References | 23 |
| Glossary | 25 |

List of Figures

| Figure | Page |
|--|------|
| 1. Probability of Observing Any Values Greater Than $K\sigma$ | 4 |
| 2. Model PDF for Single Reference Receiver, $E_L = 2.58\sigma$ –Idealized | 8 |
| 3. Tail Uncertainty Factor Verifiable for Confidence = 0.90 versus Number of Samples | 11 |
| 4. Probability Density Uncertainty Factor Verifiable for Confidence = 0.90 versus Number of Samples | 12 |
| 5. Model PDF for Single Reference Receiver, $E_L = 2.58\sigma$ –Confidence = 0.90, Number of Samples = 2,000 | 13 |
| 6. CDF Bounding of Model by Gaussian After Convolution (INF = 2.07) for $M = 3$ Reference Receivers, $E_L = 2.58\sigma$, Confidence = 0.90, Number of Samples = 2,000 | 15 |
| 7. Sigma Inflation Factor versus Number of Samples for $E_L = 1.96\sigma$ or 2.58σ , Confidence = 0.90 | 16 |
| 8. Sigma Inflation Factor versus Number of Samples, for $E_L = 1.96\sigma$, Confidence = 0.90 or 0.99 | 18 |

Section 1

Introduction

Background

The FAA's Local Area Augmentation System (LAAS) broadcasts differential corrections for each visible satellite, which are the average of corrections from M reference receivers. A quantity σ_{pr_gnd} is also broadcast to describe the error in the corrections due to the LAAS Ground Facility (LGF). Since a separate value of σ_{pr_gnd} is broadcast for each satellite, the correction errors are characterized in the range domain. In the aircraft using LAAS, protection levels are computed to bound the navigation error in the position domain that results from the broadcast corrections and other error sources such as in the avionics and data latency. These protection levels assume that the position error distribution is overbounded by a Gaussian distribution with standard deviation (herein referred to as $\sigma_{vert(M)}$) derived from the broadcast values of σ_{pr_gnd} and the geometry of the satellites being used for navigation. One such bound known as VPL_{H0} [1] is given for Category I (CAT I) and $M = 3$ reference receivers by

$$VPL_{H0} = 5.81 \times \sigma_{vert(M)} \quad (1)$$

The probability associated with VPL_{H0} is

$$\text{Probability}\{\text{Vertical Error Exceeds } VPL_{H0}\} = Q(5.81) = 3.1 \times 10^{-9} \quad (2)$$

where Q is the tail probability (single sided) for a Gaussian distribution with $\sigma = 1.0$. Thus, the vertical position error is assumed to exceed VPL_{H0} with an extremely small probability.

A significant challenge is associated with verifying that the broadcast values of σ_{pr_gnd} do in fact provide the assumed bound. An extremely large amount of data would be needed to observe and precisely characterize the tails of the error distribution. Moreover, the tails of the error distribution may not be Gaussian. A general approach to this challenge has been proposed and investigated by a number of researchers. In this approach, an estimate of the standard deviation (herein referred to as $\sigma_{pr_gnd_estimate}$) is computed from observed values of the error. An inflation factor (herein referred to as INF) is then applied to give the broadcast value as

$$\sigma_{\text{pr_gnd}} = \text{INF} \times \sigma_{\text{pr_gnd_estimate}} \quad (3)$$

The value of an INF is determined so that the assumed bound is theoretically provided. An example of inflation factors (INFs) derived using this approach may be found in [2]. The work in [2] considers the correlation between reference receivers when averaging corrections in the range domain, and the effect of satellite geometry when converting from the range domain to the position domain. However, the results in [2] are all based on assuming that the entire error distribution is Gaussian.

Purpose and Organization of This Paper

This paper develops a synthetic model for characterizing the ground error distribution if the tails are not known to be Gaussian and derives corresponding values of INF for inflating the value of $\sigma_{\text{pr_gnd}}$ to be broadcast. The paper begins with a more detailed review of the challenge associated with gathering large numbers of independent samples to characterize LAAS errors with confidence. Next, an overview of the proposed method for determining the error distribution and values of INF is presented. Then follows the details of the development of the synthetic error distribution for a single reference receiver. Hypothesis tests to verify parameters of the model distribution from data are then discussed. Then, performance tradeoffs related to analysis point and confidence level are illustrated. The paper concludes with a summary and recommendations.

Section 2

Collecting Data to Characterize Probabilities

Independent Samples of LAAS Error

It is well known that large amounts of data are needed to characterize probability distributions with confidence. The number of independent samples available for characterizing LAAS errors is limited by several factors. Differential corrections are broadcast at a 2 Hz rate (for CAT I). However, they have been computed from code measurements smoothed by carrier phase measurements in a complementary filter with a 100 s time constant. A rule of thumb is to space samples two time constants apart to achieve acceptable independence. Thus, only 18 samples are available per satellite per hour because of code-carrier smoothing. The reference receiver antennas should be sited such that those errors caused by multipath are uncorrelated among them. In that case, data from all M reference receivers can be used to maximize the number of independent samples. Thus, if roughly 7.5 satellites are typically visible and $M = 3$ reference receivers, the total number of error samples available in one day is approximately

$$18 \text{ per hr} \times 24 \text{ hrs} \times 7.5 \text{ sats visible} \times 3 \text{ references} \sim 9,720 \text{ independent samples per day} \quad (4)$$

A value of $\sigma_{\text{pr_gnd}}$ is broadcast for each individual satellite. For a multipath limiting antenna it is conceivable that $\sigma_{\text{pr_gnd}}$ may be nearly constant with elevation and the data from all satellites may be combined independent of elevation. However, in general it will be necessary to estimate $\sigma_{\text{pr_gnd}}$ in multiple elevation bins. If elevations between 5 and 90 degrees (deg) are divided into bins 1 to 5 deg wide, the number of samples per bin per day is

$$\frac{9,720}{85/1} \sim 100 \text{ to } \frac{9,720}{85/5} \sim 500 \text{ independent samples per bin per day} \quad (5)$$

A second factor limiting the number of independent samples is ground multipath at the LAAS reference antennas. Such multipath may repeat as the satellite ground trace repeats each day. Variations in satellite orbits and ground conditions may cause multipath to be independent after several days to several weeks. Thus, if one or two weeks are skipped between samples, the number of samples available per year is roughly

$$25 \times 100 = 2,500 \text{ to } 50 \times 500 = 25,000 \text{ independent samples per bin per year} \quad (6)$$

Chance of Observing Rare Values

The general problem of even observing any values with small probability of occurrence is illustrated quantitatively in Figure 1. The figure shows the probability of observing any (one or more) values beyond a given limit of $K\sigma$ versus the number of independent samples taken. The results are based entirely on the probability P that such a value could be observed on any one sample. Note that if the number of samples available is on the order of 10,000, there is a good chance of making some observations beyond values of $K\sigma$ up to $K = 3.72$ ($P = 0.0001$). However, in the case of LAAS VPL_{H0} , the interest is in the tails of the error distribution in the vicinity of 5.81σ and beyond. Note that many more samples than 10^5 are needed to have a good chance of observing even one sample greater than 5.81σ . Therefore, it is obviously not practical to directly observe and characterize the tails of the LAAS error distribution in the region of interest for VPL_{H0} .

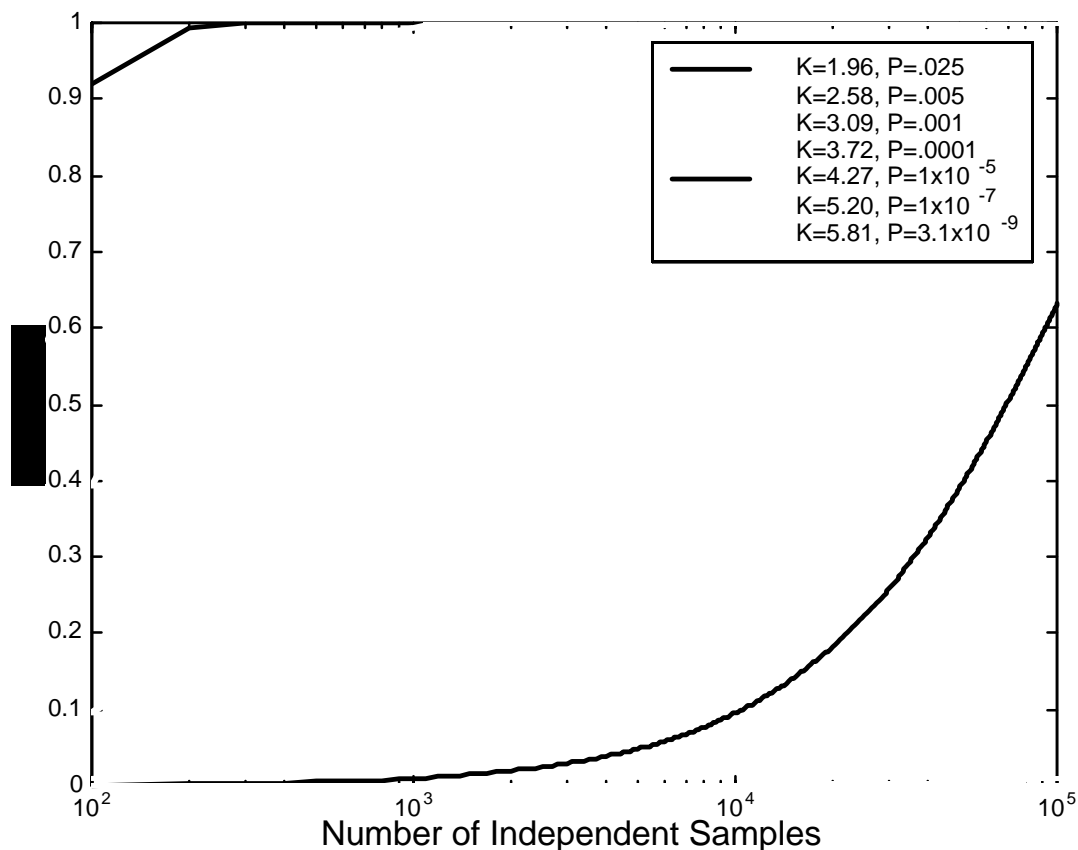


Figure 1. Probability of Observing Any Values Greater Than $K\sigma$

Section 3

Overview of Proposed Bounding Method

The major steps in the proposed bounding method are as follows:

1. The error for the correction from a single reference receiver is characterized. This involves estimating the standard deviation of the error (denoted $\sigma_{rr_estimate}$) from the maximum over all reference receivers. A corresponding model PDF for the core and tails of the error distribution is generated based on $\sigma_{rr_estimate}$. Parameters of the model are then verified by statistical hypothesis tests.
2. The error for the broadcast correction averaged over M reference receivers is derived. Assuming that the errors are uncorrelated between reference receivers, the PDF of the error in the average is the convolution of M single reference receiver PDFs. The corresponding standard deviation of the error in the average correction is $\sigma_{rr_estimate} / \sqrt{M}$.
3. The value of INF is found for $\sigma_{pr_gnd} = INF * \sigma_{rr_estimate} / \sqrt{M}$ such that the Gaussian error bound is provided at the $5.81\sigma_{pr_gnd}$ point on the tail of the error distribution for a single satellite in the range domain.
4. Corresponding bounding is assumed to be provided in the position domain (e.g., at $5.81 * \sigma_{vert(M)}$). A similar bounding relationship involving the entire distribution has been shown to be true [3] if the error distribution is zero mean, symmetric about zero, and unimodal. Bounding for each satellite is also conservative except in the case where the geometry is such that a single satellite dominates the transformation of the error from the range domain to the position domain.

The remainder of the paper focuses on the first three steps above to generate a bounding PDF and corresponding INF for the average correction for a single satellite.

Section 4

Model For Error of Single Reference Receiver

Steps in Generation and Verification

The major steps in the generation and verification of the model PDF are:

1. The value of $\sigma_{rr_estimate}$ is computed from observed data.
2. An analysis point $E_L = K_L * \sigma_{rr_estimate}$ is selected so that the probabilities of the PDF and tail at E_L are significantly larger than at 5.81σ . This paper illustrates the method for values of K_L equal to 1.96 and 2.58.
3. The core of the distribution (errors with magnitude not exceeding E_L) is verified to be Gaussian with standard deviation $\sigma_{rr_estimate}$. This verification of the core may be performed using well-known goodness-of-fit tests [4, chapter 4] such as the χ^2 test on the PDF or the Kolmogoroff-Smirnoff (Lilliefors) test on the cumulative distribution function (CDF).
4. The PDF at E_L is verified to be the Gaussian value $g(E_L)$ using a statistical hypothesis test. For example, for a Gaussian distribution, the probability of occurrence in a 0.33σ wide bin centered at 2.58σ is $0.33 * g(2.58\sigma) = 0.33 * 0.0146 \sim 0.0049$.
5. The tail probability beyond E_L is verified to be the Gaussian value $P_t(E_L)$ using a statistical hypothesis test. For example, the single-sided tail probability of a Gaussian distribution beyond 2.58σ is $P_t(2.58\sigma) = 0.005$.
6. For values of E beyond E_L in magnitude, the PDF is assumed to be Laplacian (sometimes referred to as “double exponential”) given by equation (7). The Laplacian and Gaussian are two members of the family of PDFs that involve raising e to the negative of the argument itself raised to a power A . For the Gaussian $A = 2$ and for the Laplacian $A = 1$. In lieu of direct knowledge that the tail is Gaussian, the Laplacian is chosen to be more conservative, since it decreases much more slowly as the size of the error increases.

$$p(E) = g(E_L) \times \exp\left(-\frac{|E - E_L| \times g(E_L)}{P_t(E_L)}\right); |E| \geq E_L \quad (7)$$

Idealized Error Model Probability Density Function

Figure 2 shows the synthetic model PDF for a single reference receiver for $E_L = 2.58\sigma$. Note the tail decreases much more slowly than the Gaussian PDF for the tail beyond E_L . This PDF is referred to as “idealized,” because it is constructed without regard for the extent to which it can be verified by tests on data.

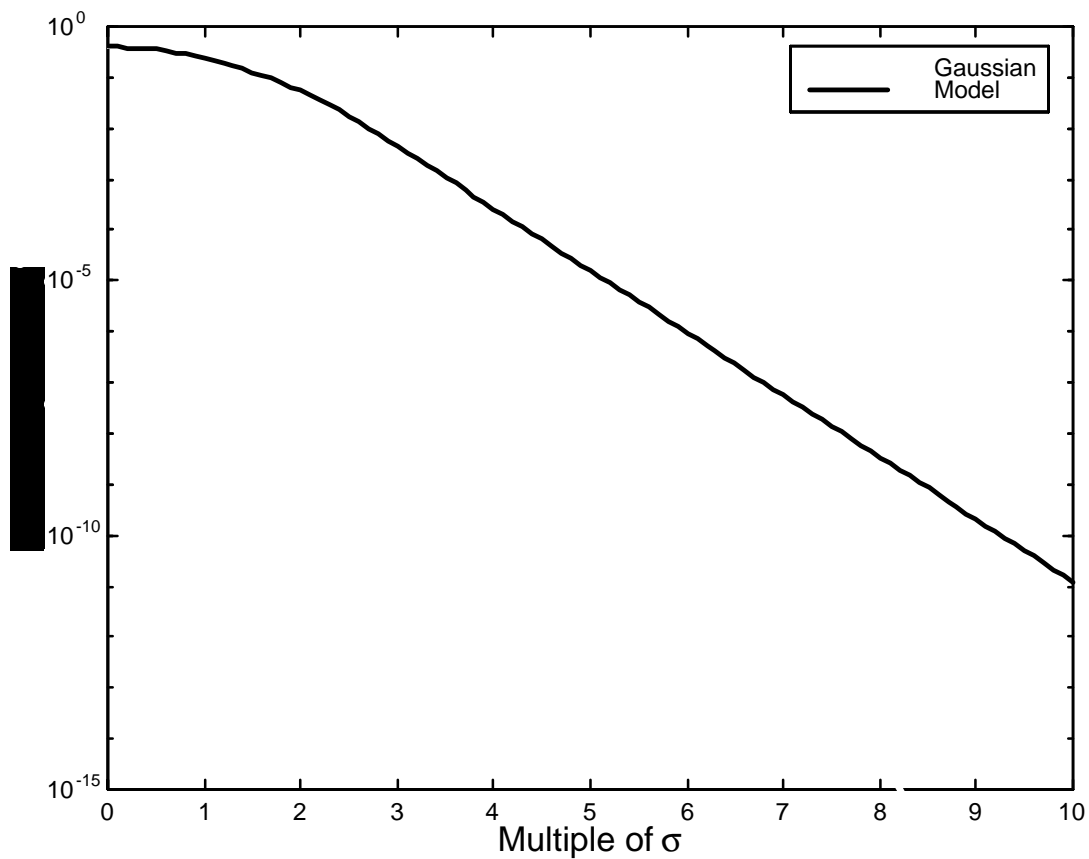


Figure 2. Model PDF for Single Reference Receiver, $E_L = 2.58\sigma$ –Idealized

Section 5

Hypothesis Tests

General Performance Characteristics

Recall that the method uses hypothesis tests to verify that the PDF at E_L and the tail probability beyond E_L are the Gaussian values. The hypothesis test concept will be illustrated in the context of verifying that the tail probability does not exceed some value p_0 . This involves examining N observed independent samples of the error and determining how many exceed E_L . If the samples may be regarded as independent trials with probability p_0 of exceeding E_L on each trial, the probability of exactly R samples exceeding E_L in N trials is given by the well-known binomial distribution

$$P_{\text{binom}}(N, R, p_0) = \frac{N!}{R!(N-R)!} (p_0)^R (1-p_0)^{(N-R)} \quad (8)$$

The probability that S or fewer samples will exceed E_L is given by the cumulative binomial distribution

$$P_{\text{cbinom}}(N, S, p_0) = \sum_{j=0}^S P_{\text{binom}}(N, j, p_0) \quad (9)$$

The probability that more than S samples will exceed E_L is thus given by

$$\text{Pr ob}\{\text{more than } S \text{ samples exceed } E_L\} = 1 - P_{\text{cbinom}}(N, S, p_0) \quad (10)$$

The number of samples observed to be greater than E_L (denoted N_g) is compared to the test threshold T . If $N_g > T$, the hypothesis that the tail probability = p_0 is rejected. T is chosen so that the probability the test will fail even if the tail probability = p_0 is limited to a small value α . This probability of false rejection (also known as probability of Type I error) is given by

$$\text{Prob}\{\text{false rejection}\} = \text{Prob}\{\text{Type I error}\} = \alpha = 1 - P_{\text{cbinom}}(N, T, p_0) \quad (11)$$

The threshold T is chosen to give $\alpha = 0.05$. Thus, if $p = p_0$, there is a 0.95 probability the test will pass. Of course, if $p < p_0$, the probability the test will pass is greater than 0.95.

If the actual tail probability is some value $p_1 > p_0$, there is still some probability the test could pass. This situation is known as false acceptance or Type II error. The probability of this happening is given by

$$\text{Prob}\{\text{false acceptance}\} = \text{Prob}\{\text{Type II error}\} = \beta = P_{\text{cbinom}}(N, T, p_1) \quad (12)$$

The value of $p_1 = p_c$ for which β is a desired level (e.g., 0.1) can be determined using equation (12). Tail probabilities $\geq p_c$ will be rejected with probability at least $1 - \beta = 0.90$. Thus, such a test provides 0.90 confidence that the tail probability does not exceed p_c .

Since two hypothesis tests are conducted, both must pass to accept an error distribution with characteristics deviating significantly from those assumed. The tail test is on samples exceeding E_L and the PDF test is on samples in a bin centered at E_L . Thus, the tests are considered to be independent and the probability of both tests passing is the product of the probabilities of the individual tests passing. Therefore, to achieve an overall probability of Type II error equal to β , the Type II error allocated to each individual test is

$$\text{Prob}\{\text{Type II error per test}\} = (\text{Prob}\{\text{Overall Type II error}\})^{1/2} = \beta^{1/2} \quad (13)$$

Probability Uncertainties That Can Be Verified

For the purpose of illustrating test performance, it is convenient to define an uncertainty factor relating the probability that can be verified with given confidence to the probability assumed by the hypothesis. For the tail probability hypothesis test, a tail uncertainty factor (TUF) is defined by

$$(\text{tail probability verified with given confidence}) = \text{TUF} \times (\text{hypothesized tail probability}) \quad (14)$$

A graph of TUF versus the number of independent samples is given in Figure 3. The values of TUF are for overall confidence = 0.90 from the two tests ($\beta = 0.1^{1/2} \sim 0.31$ from each individual test). Two curves are shown corresponding to values of $E_L = 1.96\sigma$ and 2.58σ . To understand the implications of the graph, consider the points for 2,000 samples. If the analysis is done at $E_L = 2.58\sigma$, a probability as large as 1.76 times the hypothesized

value (0.005) can be protected against with 0.90 confidence. On the other hand, if the analysis is done at $E_L = 1.96\sigma$, the 0.90 confidence is provided for protecting against a probability as large as 1.33 times the hypothesized value (0.025). The TUF is smaller for 1.96σ than for 2.58σ because the overall probability being tested is much larger at 1.96σ . As would be expected, as the number of samples increases, the values of TUF decrease. Having more independent samples improves the ability of the test to discriminate between the hypothesized tail probability and a larger value. A TUF = 1.0 would occur for an infinite number of samples, corresponding to perfect protection for a probability exactly equal to the hypothesized value.

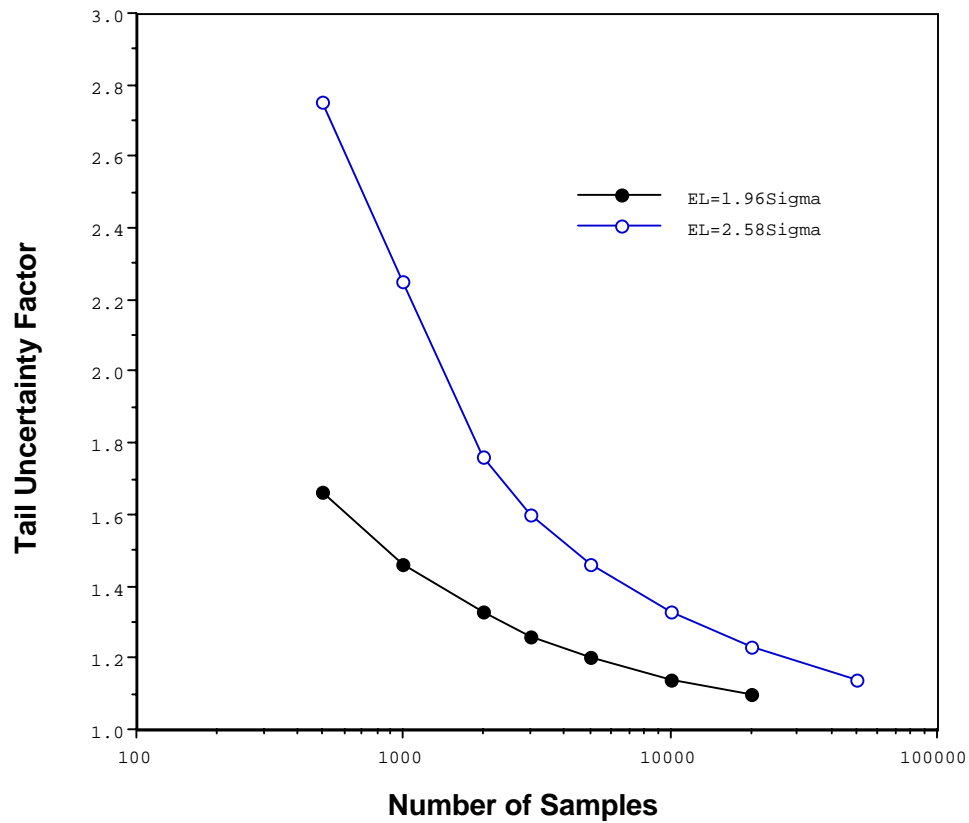


Figure 3. Tail Uncertainty Factor Verifiable for Confidence = 0.90 versus Number of Samples

A probability density uncertainty factor (PUF) is defined for the PDF test by

$$(\text{bin probability verified with given confidence}) = \text{PUF} \times (\text{hypothesized bin probability}) \quad (15)$$

The dependence of PUF on the number of independent samples is shown in Figure 4. As for TUF, the overall confidence is 0.90 and two curves are shown for $E_L = 1.96\sigma$ and 2.58σ . The graph shows results for PUF smaller than 1.0 (rather than larger than 1.0 as for TUF). To understand the reason for this, refer back to equation (7) defining the Laplacian tail for the model error distribution. Note that for increasing values of E , the tail falls off more slowly for smaller values of the PDF value $g(E_L)$ being matched by the model. Therefore, it is desirable to protect against values of the PDF that are smaller than the hypothesized value. Consequently, better performance is achieved with PUF increasing toward 1.0 as the number of independent samples increases. Again, the values of PUF that are protected for $E_L = 1.96\sigma$ are better than those protected for $E_L = 2.58\sigma$ because the absolute probabilities are larger at 1.96σ .

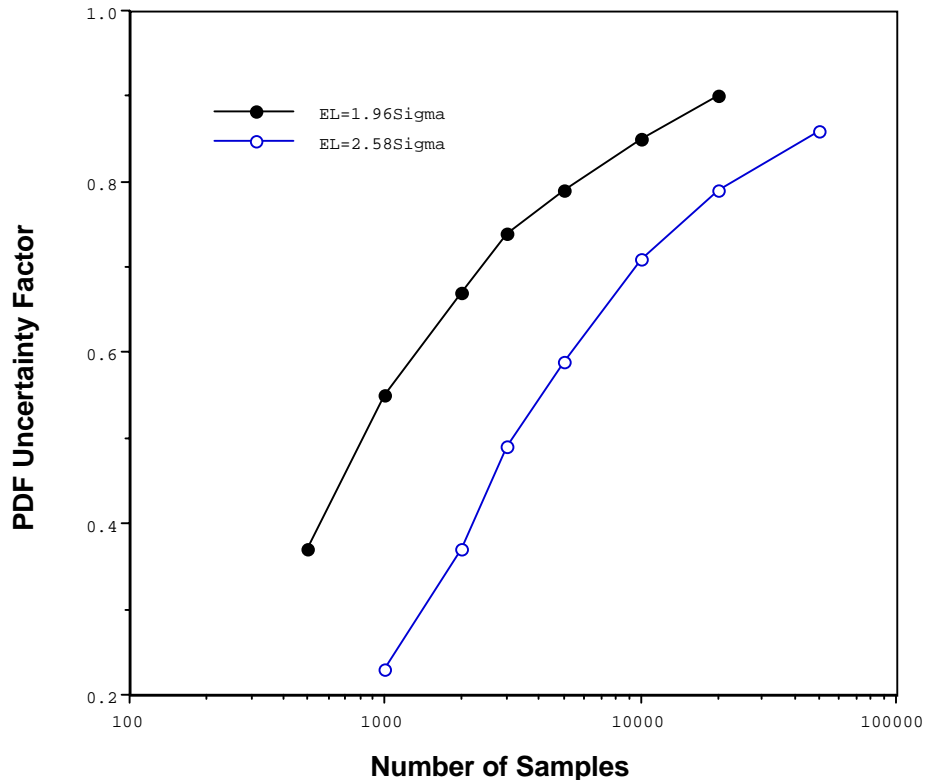
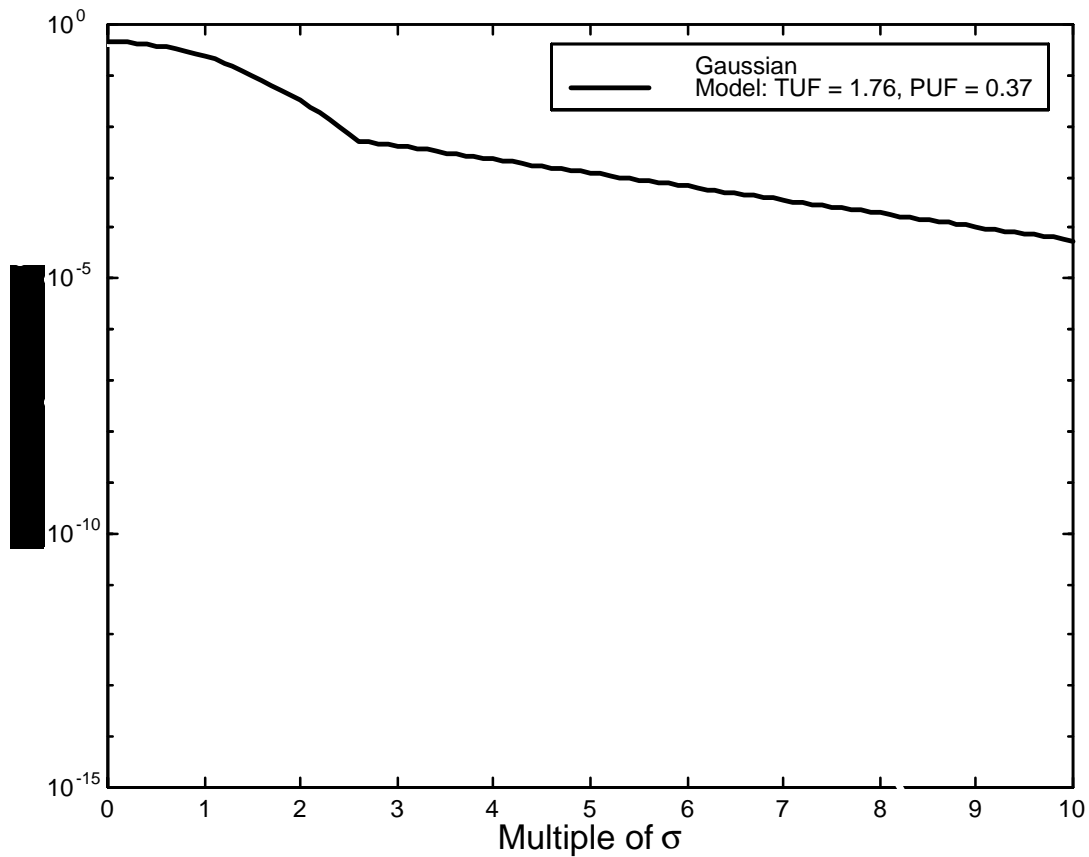


Figure 4. Probability Density Uncertainty Factor Verifiable for Confidence = 0.90 versus Number of Samples

Verifiable Error Model Probability Density Function

An example of an error model PDF that can be verified with a given confidence is shown in Figure 5. This PDF is derived using values of TUF = 1.76 and PUF = 0.37 that can be protected with total confidence = 0.90 when 2,000 independent samples are observed. Note that in comparison to the idealized PDF in Figure 2, the verifiable PDF in Figure 5 falls below the Gaussian for some range of values of E less than 2.58σ but rises slightly higher than the Gaussian for values of E near 0. Thus, the model PDF also qualitatively accounts for uncertainty in verifying that the core of the distribution is Gaussian. Note also that the tail beyond 2.58σ is significantly higher than in Figure 2, corresponding to the uncertainties in the PDF and tail probabilities that can be verified.



**Figure 5. Model PDF for Single Reference Receiver, $E_L = 2.58\sigma$ —
Confidence = 0.90, Number of Samples = 2,000**

Section 6

Inflation Factor Results

Example of Cumulative Distribution Function (Tail) Bounding

Recall that the inflation factor INF multiplying $\sigma_{pr_gnd_estimate}$ to compute σ_{pr_gnd} is determined so that a Gaussian CDF using σ_{pr_gnd} bounds the CDF of the error in the average correction at the $5.81\sigma_{pr_gnd}$ point. The PDF of the error in the correction derived from averaging M reference receivers is determined by convolving M copies of the model PDF for a single reference receiver. An example of this bounding for M = 3 and using the model PDF from Figure 5 is given in Figure 6. An INF of 2.07 is required to achieve the bounding shown. Although not illustrated in this paper, it should be pointed out that the tails of the model PDF are reduced significantly by the convolution operation. Therefore, if the verification of probabilities through hypothesis tests were to be done on the correction error after averaging (rather than at the individual reference receiver level), the resulting INFs would be significantly larger.

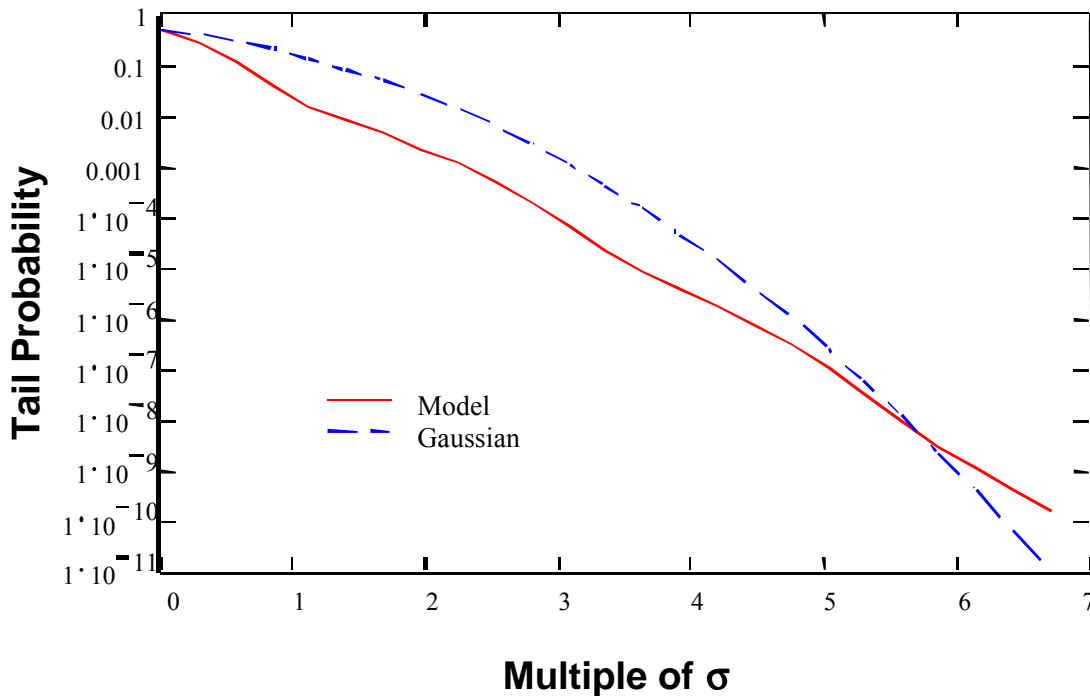


Figure 6. CDF Bounding of Model by Gaussian After Convolution (INF = 2.07) for M = 3 Reference Receivers, $E_L = 2.58\sigma$, Confidence = 0.90, Number of Samples = 2,000

Variation of Inflation Factor with Number of Samples

Figure 7 shows the variation of INF with the number of independent samples for confidence 0.90. Curves are plotted for $E_L = 1.96\sigma$ and 2.58σ . As expected, the INFs are smaller if more independent samples are available for analysis. The INFs increase dramatically when the number of samples falls below several thousand. Note that the curve for 2.58σ is even higher than the curve for 1.96σ . At first consideration, this does not seem correct, because doing the analysis at a smaller multiple of σ requires extrapolating the Laplacian model for a longer distance out to the bounding point of 5.81σ . However, referring back to Figures 3 and 4 reveals that smaller relative probability uncertainties can be verified more easily at 1.96σ . Therefore, the net result is smaller INFs when both the

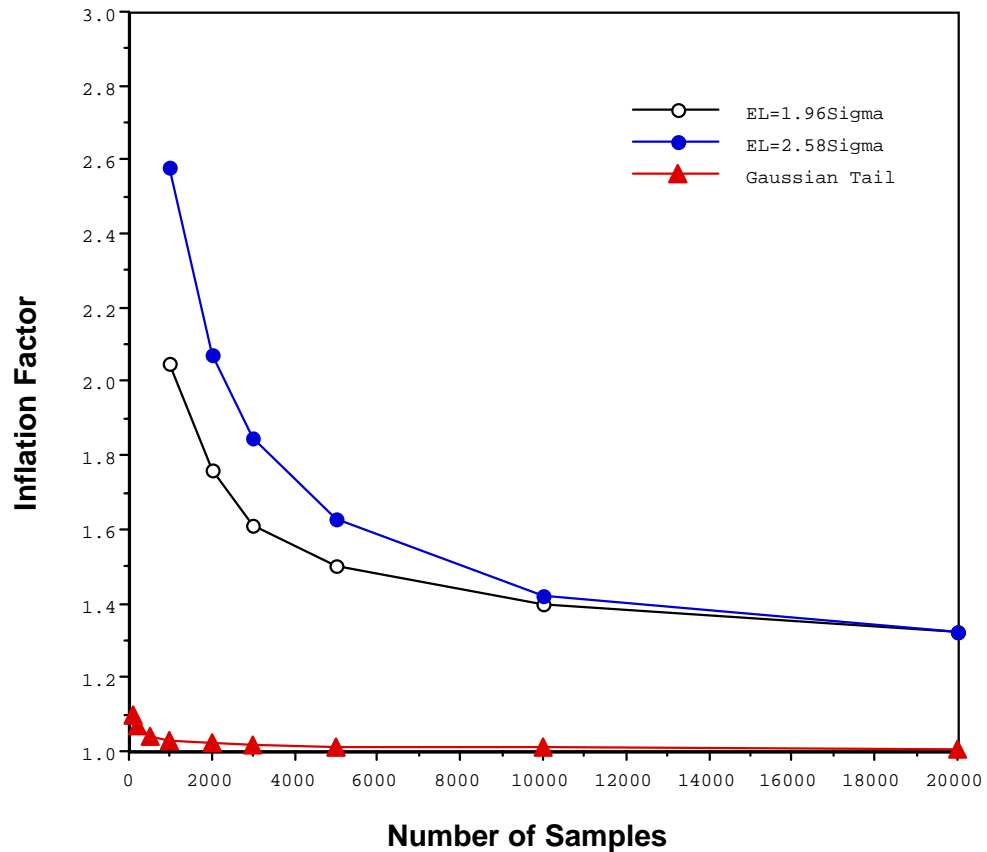


Figure 7. Sigma Inflation Factor versus Number of Samples for $E_L = 1.96\sigma$ or 2.58σ , Confidence = 0.90

extrapolation distance and the probability uncertainty effects are taken into account. The graph also shows a third curve corresponding to assuming the error PDF is Gaussian in the tails. For that case INF is just the upper confidence limit for estimating the square root of the sample variance from a limited number of samples. Results are computed using the well-known χ^2 distribution (see [4], Chapter 4). Note that significantly smaller INFs can be used if the tails of the error distribution are known to be Gaussian.

Variation of Inflation Factor with Confidence

Figure 8 shows values of INF for confidence = 0.99 in addition to values for confidence = 0.90 previously illustrated. Note that when the number of samples is relatively large, INF is not much greater for the higher confidence. However, for fewer than several thousand samples, INF increases significantly when the confidence is increased from 0.90 to 0.99. Determining the minimum level of confidence required is beyond the scope of this paper. However, these results indicate that intolerably large INFs would be associated with confidence higher than 0.99 for less than a few thousand samples.

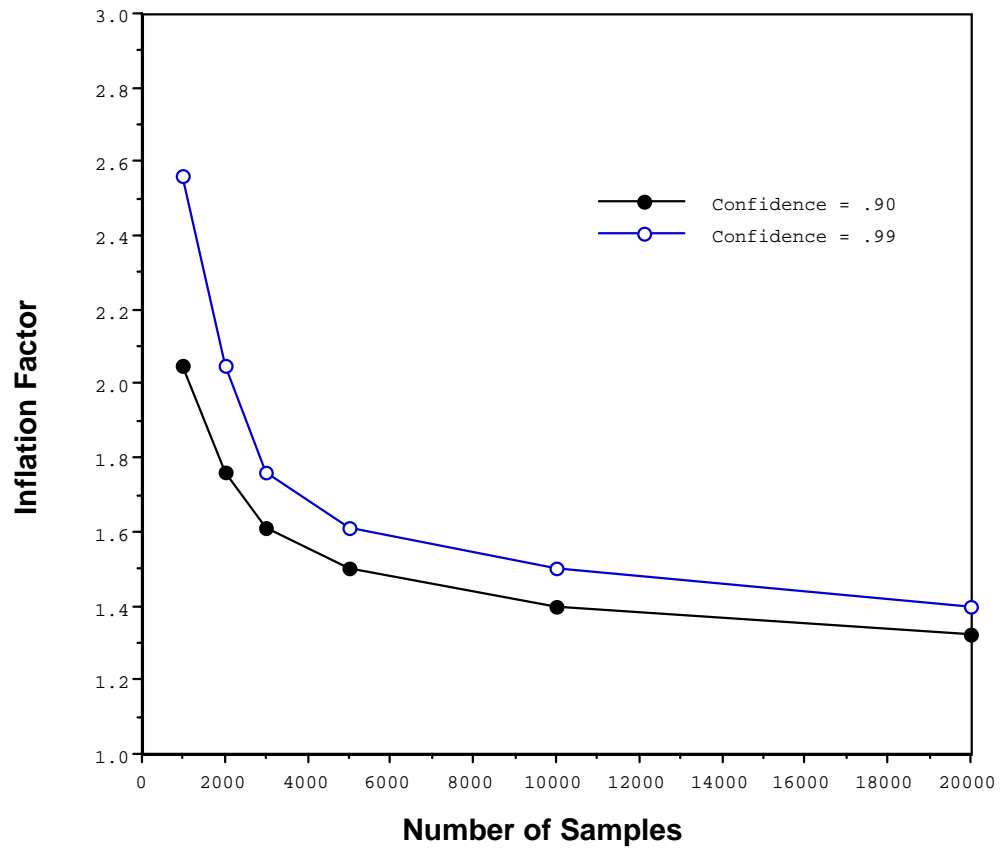


Figure 8. Sigma Inflation Factor versus Number of Samples, for $E_L = 1.96\sigma$, Confidence = 0.90 or 0.99

Section 7

Summary

- LAAS broadcasts σ_{pr_gnd} to characterize the errors in the differential corrections of each satellite. The aircraft computes a high probability bound on position error assuming the ground errors are Gaussian distributed with standard deviation σ_{pr_gnd} .
- Verifying from data that LAAS achieves such a bound is difficult because the number of independent samples is limited by correlation caused by smoothing and multipath that repeats daily. In addition, the tails of the error distribution may not be Gaussian.
- A synthetic model is developed for the probability density function of the error from a single reference receiver using a Gaussian core but Laplacian tails. The probability density function of the error in the correction averaged over multiple receivers is constructed from this model by convolution.
- Hypothesis tests are developed for analyzing data to verify parameters of the model probability density and tail probability with known confidence.
- Corresponding values of an inflation factor are developed to increase the broadcast value of σ_{pr_gnd} so that the bounding is achieved using the Gaussian cumulative distribution function assumed in the aircraft.
- Even with several thousand samples, the resulting inflation factors provide limited confidence and are significantly larger than would be needed if the tails of the error distribution were known to be Gaussian.

Section 8

Recommendations

- Apply the method to data to characterize the error as far out on the tails of the distribution as possible.
- Recognize that an inflation factor can be used that is initially large but may be decreased as more measurements are made and more experience is gained.
- Continue efforts to establish physical arguments that the tails of the ground error distribution are Gaussian.
- Consider revising the application of VPL_{H0} to be an accuracy test at the 95-percent level (as in conventional navigation systems) rather than an integrity test at the 5.81σ level.

List of References

1. RTCA, Minimum Aviation System Performance Standards for the Local Area Augmentation System (LAAS), RTCA/DO-245, September 28, 1998, RTCA Inc., Washington, DC.
2. Pervan, B. and I. Sayim, “Issues and Results Concerning the LAAS σ_{pr_gnd} Overbound,” presented at IEEE Position Location and Navigation Symposium (PLANS) 2000, San Diego, CA, 13–16 March 2000.
3. DeCleene, B., “Proof for ICAO Overbounding Requirement,” attachment B to *Protection Level and Overbounders Subgroup Report* by T. Murphy, ICAO GNSSP/WG-B WP24, Canberra, Australia, 17–18 January 2000.
4. Sachs, L., *Applied Statistics*, Springer-Verlag, New York, NY, 1982.

Glossary

| | |
|--------------|--|
| CAT I | Category I |
| CDF | cumulative distribution function |
| FAA | Federal Aviation Administration |
| INF | inflation factor |
| LAAS | Local Area Augmentation System |
| LGF | LAAS Ground Facility |
| PDF | probability density function |
| PUF | probability density uncertainty factor |
| TUF | tail uncertainty factor |

Distribution List

Internal

F018

A. N. Sinha, asinha@mitre.org

F020

J. K. Reagan, jreagan@mitre.org
R. Swensson, W372, rswensso@mitre.org

F040

F. Petroski, W300 (frp@mitre.org)

F060

L. Ryals, W300 (ryals@mitre.org)

F080

R. Braff, rbraff@mitre.org
J. Chadwick, W300 (chadwick@mitre.org)
A. Steger, W300 (asteger@mitre.org)

F082

J. N. Barrer, jbarrer@mitre.org
E. Q. Calle, emily@mitre.org
H. L. Crane, lescrane@mitre.org
M. B. El-Arini, bakry@mitre.org
S. D. Ericson, ericson@mitre.org
J. P. Fernow, jfernow@mitre.org
C. J. Hegarty, chegarty@mitre.org and Chris.Hegarty@faa.gov
T. T. Hsiao, thsiao@mitre.org
T. Kim, tkim@mitre.org
Y. C. Lee, ylee@mitre.org
R. O. Lejeune, rlejeune@mitre.org
K. R. Markin, kmarkin@mitre.org
S. V. Massimini, svm@mitre.org
M. McLaughlin, mpmcl@mitre.org
D. G. O'Laughlin, danielo@mitre.org
W. A. Poor, wpoor@mitre.org
K. S. Sandhoo, kan@mitre.org
W. C. Scales, wscases@mitre.org
J. L. Schwartz, jschwartz@mitre.org
C. A. Shively, cshively@mitre.org (10 copies)
M. Tran, mtran@mitre.org
C. C. Varner, ccvarner@mitre.org
M. J. Zeltser, mzeltser@mitre.org

F082 project file (4 copies)*
F082 correspondence file (1 copy)*

F084

P. Hegarty, W306 (phegarty)

Records Resources (2)

External

John Mills, AND-210, John.Mills@faa.gov*
David Olsen, ASD-140, David.Olsen@faa.gov*
Hal Bell, AND-730, Hal.Bell@faa.gov
Robert J. Bernard, ASD-10, Bob.Bernard@faa.gov
Deane Bunce, AND-730, Deane.Bunce@faa.gov
Hank Cabler, AFS-430, Hank.Cabler@faa.gov
Bruce DeCleene, AIR-130, Bruce.DeCleene@faa.gov
Maria DiPasquantonio, AND-730, Maria.DiPasquantonio@faa.gov
Leo Eldredge, AND-730, Leo.Eldredge@faa.gov
Norm Fujisaki, ASD-2, Norm.Fujisaki@faa.gov
Dan Hanlon, AND-730, Dan.Hanlon@faa.gov
Mike Harrison, ASD-100, Michael.Harrison@faa.gov,
D'Borah Hart, SVC-123.20, D'Borah.Hart@faa.gov:
(FAA librarian: 2 copies + 1 electronic copy)
Steve Hodges, AND-730, Steve.Hodges@faa.gov
Jon Jordan, AND-730, Jonathan.CTR.Jordan@faa.gov
Harry Kane, AND-700, Harry.Kane@faa.gov
Barbara Lingberg, AND-730, Barbara.Lingberg@faa.gov
Jack Loewenstein, AND-700, Jack.Loewenstein@faa.gov
Carl Marquis, ASR-1, Carl.Marquis@faa.gov
Jean E. Mills, ASD-600, (letter only) Jean.Mills@faa.gov (letter only)*
Dave Peterson, AND-730, Dave.Peterson@faa.gov
Carlos Rodríguez, AND-730, Carlos.Rodriguez@faa.gov
John Scardina, ASD-1, John.Scardina@faa.gov
Gary Skillicorn, AND-702, Gary.Skillicorn@faa.gov
Jim Snow, AVN-5, James.Snow@faa.gov
Ann Tedford, ASD-140, Ann.Tedford@faa.gov
Ted Urda, AND-730, Ted.Urda@faa.gov

Federal Aviation Administration
800 Independence Avenue, SW
Washington, DC 20591

Bill Wanner, ACT-360, Bill.Wanner@faa.gov
John Warburton, ACT-360, John.Warburton@faa.gov
Victor Wullschleger, ACT-360, Victor.Wullschleger@faa.gov

William J. Hughes Technical Center,
Building 301, Room 305,
Atlantic City International Airport,
Atlantic City, NJ 08405

Frank van Graas, vangraas@ohiou.edu
Ohio University
Avionics Engineering Center
Stocker Center
Athens, OH 45701-2979

Per Enge, per@relgyro.Stanford.edu
Hansen Labs/GP-B
Stanford University
Stanford, CA 94305-4085

Barbara Clark, clarkbs@navair.navy.mil
NAWCAD
Bldg 1641, MS-3
21871 Nickler Rd
Patuxent River, MD 20670

Boris Pervan, pervan@iit.edu
Illinois Institute of Technology
2526 Engineering Bldg
10 West 32nd St
Chicago, IL 60616-37